

SCIENTIFIC PAPERS  
OF THE UNIVERSITY OF PARDUBICE  
Series A  
Faculty of Chemical Technology  
17 (2011)

**EFFECT OF SURFACE ROUGHNESS  
ON SURFACE FREE ENERGY OF COATED PAPERS**

Marie KAPLANOVÁ<sup>1</sup>, Jan VALIŠ Bohumil JAŠÚREK and Tomáš SYROVÝ  
Department of Graphic Arts and Photophysics,  
The University of Pardubice, CZ–532 10 Pardubice

Received September 30, 2011

*The surface properties of two sets of coated printing papers were studied by the monitoring of the dynamic behaviour of small drop of standard liquid (water, ethylene glycol, formamide and methylene iodide) in time region of 20 s after drop impact on solid surface (“sessile“ drop method). The contact angle  $\theta$  formed by a liquid drop at the three-phase boundary is a quantitative measure of the wetting of a solid by a liquid. The usual goal of the contact angle measurement is the calculation of surface free energy (SFE) of solid using the semi-empirical equations including the estimation of the interfacial interaction between liquid and solid phases. Using the “cos  $\theta$  model”, pseudo-equilibrium contact angle  $\theta_{eq}$ , liquid spreading rate  $k_1$  and the rate of liquid penetration  $k_2$  were evaluated. Surface roughness was measured by profilometer and by instrument Parker Print-Surf™. The roughness values obtained by both methods correlated well. The spreading rate parameter  $k_1$  decreases and the  $k_2$  parameter increases with increasing roughness of tested papers. The topographical structure of paper samples was studied by electron microscopy. Polar and disperse components of*

---

<sup>1</sup> To whom correspondence should be addressed.

*SFE were evaluated by means of different theoretical approaches to interphase interactions (Owens–Wendt, van Oss, Good and Chaudhury and Wu). The SFE calculation based on Owens–Wendt and Wu equations resulted in much higher values of the total SFE and its polar component than the values calculated by acido-basic approach derived by van Oss et al.*

## **Introduction**

The experience of printers with the unpredictability of image quality when moving over to a printing material of the same type designation from another manufacturer suggests that the commonly used designation of papers is not sufficient. The designation of various types of printing papers as glossy, matt, satin matt or fat matt represents only a very rough indication of these materials, the interaction of which with ink and especially with low-viscosity ink can be very different. The surface energy of paper, the rate of spreading of liquid ink or varnish on the paper surface and the level of penetration of ink into the paper structure are influenced by the surface roughness, pore size and pore distribution and by the morphology and chemical composition of the pigments in the paper coating. Printers use special test fluids and various empirical methods to determine the print penetration, varnishability, and to evaluate the surface free energy of papers and prints. They, however, usually use these methods only if there is a problem, such as excessive dot gain, ink penetration through the paper on the other side, lack of luster, uneven varnishing or poor adhesion of ink or lacquer on the paper. Detailed objective characterization of the surfaces of printed materials can be useful even for advanced manufacturers of printed materials who are searching for the optimum technologies to be used in final finishing of paper surfaces.

One of the effective methods for studying the surfaces of solids is monitoring of the dynamic behaviour of a small drop of a standard liquid placed on the surface of a solid (the “sessile“ drop method). Contact angles are surface sensitive. The results obtained by this method, therefore, provide information about the smoothness and homogeneity of the solid surface and about the rate of spreading of the liquid and its penetration into the paper coating layer. It also offers the possibility to evaluate various properties of both sides of two-side coated papers as well as various properties depending on the direction of the paper coating and on the surface microstructure resulting from the coating technology. It has been shown that experimental methods and procedures similar to those that are used to evaluate the time course of the contact angle (the dynamic contact angle  $\theta(t)$ , DCA) may be also used for non-standard liquids, e.g., for non-viscous inks, and to simulate the behaviour of these inks on the printing substrate [1]. In many practical applications it is of greater importance to know the speed of the moving of three-phase contact line than the final equilibrium state.

Measurement of the time dependence of the contact angle of some liquids partially wetting solids was reported by many authors and different models explaining such dynamic properties were proposed (the molecular-kinetic theory, the hydrodynamic theory and combined models [5,9,10]). Because the drop shape changes with time, some energy dissipation can be considered: viscous dissipation in the wedge of the contact angle, frictional processes at the three-phase contact line, and so on. The achievements and limitations of the different approaches to the description of the moving wetting line lead to the conclusion that dynamic wetting remains an open area of research, with much still left to investigate.

The usual purpose of contact angle measurement in practice is the calculation of the surface free energy (SFE) of solids, using a semi-empirical equation which includes the estimation of the interfacial interaction between the liquid and the solid phase.

Three equations have been widely used to interpret the contact angle data of solids [6,7,8], each using a different approach to the evaluation of the interfacial solid-liquid tension. The first one resulted from the geometric mean approach (Owens and Wendt's method) and assumes two surface tension components (dispersive  $\gamma^d$  and polar  $\gamma^p$  interfacial tensions at the solid/vapour (SV), solid/liquid (SL) and liquid/vapour (LV) interfaces,  $i = SV, SL$  and  $LV$ , respectively)

$$\begin{aligned} \gamma_i &= \gamma_i^d + \gamma_i^p. \\ \gamma_{LV}(1 + \cos\theta_{eq}) &= 2\left(\sqrt{\gamma_{SV}^d \gamma_{LV}^d} + \sqrt{\gamma_{SV}^p \gamma_{LV}^p}\right) \end{aligned} \quad (1)$$

The geometric mean approach has been in use for more than three decades, even though some articles have been published that prove it to be incorrect [6]. The main problem is the wrong assumption that any polar materials interact only with any other polar materials as a function of their internal polar cohesive forces.

The method utilizing the harmonic mean approach to assess the dispersion and polar contribution (Wu's method) can be represented by the equation

$$\gamma_{LV}(1 + \cos\theta_{eq}) = \frac{4\gamma_{SV}^d \gamma_{LV}^d}{\gamma_{SV}^d + \gamma_{LV}^d} + \frac{4\gamma_{SV}^p \gamma_{LV}^p}{\gamma_{SV}^p + \gamma_{LV}^p} \quad (2)$$

The harmonic mean approach exhibits the same defects as the geometric mean approach.

A more advanced approach was developed by van Oss, Good and Chaudhury who estimated the free energy of the solid surface, assuming two components of surface free energy,  $\gamma^{LW}$  and  $\gamma^{AB}$

$$\gamma_{LV}(1 + \cos \theta_{eq}) = 2 \left( \sqrt{\gamma_{SV}^{LW} \gamma_{LV}^{LW}} + \sqrt{\gamma_{SV}^- \gamma_{LV}^+} + \sqrt{\gamma_{SV}^+ \gamma_{LV}^-} \right) \quad (3)$$

one component being the Lifshitz-van der Waals interactions (*LW*), comprising dispersion, dipolar and induction interactions, the other the acid-base interactions (*AB*), comprising all electron donor-acceptor interactions, such as hydrogen bonding

$$\gamma_i = \gamma_i^{LW} + \gamma_i^{AB} \quad (4)$$

where *i* represents *SV*, *SL* and *LV*, respectively. The acid-base component of surface free energy is given by

$$\gamma_i^{AB} = 2 \sqrt{\gamma_i^+ \gamma_i^-} \quad (5)$$

where  $\gamma_i^+$  is the Lewis acid parameter and  $\gamma_i^-$  the Lewis base parameter of surface energy.

The equilibrium contact angle  $\theta_{eq}$  used in all methods of SFE calculations is easy to measure on ideally smooth and homogeneous surfaces, but it is difficult to obtain it when measuring dynamic wetting on real surfaces. Some researchers use the initial contact angle  $\theta_{init} = \theta_{t=0}$  instead of  $\theta_{eq}$  [8]. Most of the experimenters measuring contact angles by commercial tensiometers use the average contact angle values, calculated from the values measured in a certain time interval after the fall of the drop on the surface, in their calculations.

The aim of our work was to contribute to the solving of two fundamental problems in determining the SFE of papers: the determination of the equilibrium contact angle and the assessment which of the empirical equations (1)-(3) leads to the most plausible results, best characterizing these materials. The roughness and/or porosity of a surface obviously affect the spreading conditions. During our previous studies of more than one hundred rubber samples [2,3] and printing substrates of different surface quality in the time interval of tens of seconds after the liquid drop hits the solid surface [1,4], we observed that the general course of time dependence of the contact angle of the test liquids can be characterized as an initially rapid and then slow gradual decrease.

The time dependence of the contact angle  $\theta$  was converted into the time dependence of  $\cos \theta$  and the experimental results were fitted by the sum of two functions:  $F_1(t)$ , describing the relatively quick spreading of the liquid, and  $F_2(t)$ , describing the slow processes as the evaporation and penetration of the liquid or its interaction with the surface of the solid. The two stages of the wetting process can be described as a superposition of the exponential function for spreading  $F_1(t) = -A \exp(-k_1 t)$  and the linear function  $F_2(t) = B + k_2 t$  for slow evaporation and penetration, where  $(B - A)$  corresponds to the cosine of the initial contact angle

$\theta_{init}$ , and the parameters  $k_1$  and  $k_2$  characterize the rate of spreading and the rate of the process of evaporation of the liquid and/or its penetration into the substrate, respectively

$$\cos \theta = F(t) = F_1(t) + F_2(t) = -Ae^{-k_1 t} + k_2 t + B \quad (6)$$

We assume that the state of the minimum free energy will be reached at the end of the spreading stage when  $F_1(t) \rightarrow 0$ . On the basis of this assumption, the corresponding time moment  $t_{eq}$  and the respective contact angle  $\theta_{eq}$  can be estimated.

The proposed model is defined by four parameters — the amplitudes  $A$  and  $B$  and the rate parameters  $k_1$  and  $k_2$ . It was experimentally tested which properties of liquids and solids (surface tension, viscosity, density and evaporation rate of liquids, surface roughness and type of coating of papers) affect the rate parameters  $k_1$  and  $k_2$ . A method of evaluating the equilibrium (pseudo-equilibrium) contact angle  $\theta_{eq}$  and other characteristics was proposed and verified (the detailed description of our proposed model is described in Refs [1,4]).

## Experimental Materials and Methods

The subject of our study was two sets of both-side, double coated printing papers, Hello (Sappi Papier Holding, Austria) and Core (Ospap, CR), the basis weight of which was  $115 \text{ g m}^{-2}$ . The surface roughness of the samples was measured by the Mitutoyo SurfTest SJ-301 profilometer, working with the sampling length of 0.8 mm. Two parameters were considered — the arithmetical mean roughness  $R_a$  and the ten-point mean roughness  $R_z$ . The surface roughness  $R_a$  is given as the arithmetical mean value for a randomly sampled area. In the case of  $R_z$ , a section of standard length is sampled from the mean line on the roughness chart and the distance between the mean line and the peaks and valleys is measured. The parameter  $R_z$  is defined as the sum of two values: the average peak among the five tallest peaks and the average valley among the five deepest valleys.

*PPS* roughness of the papers was measured using the Parker Print-Surf™ (Messmer Bücher) instrument, which is designed to accurately measure the surface roughness of sheet materials under conditions similar to those experienced during the printing process. The sample is clamped between a precision engineered measuring head and a specifically designed backing assembly. The resistance to airflow is measured and converted into the mean roughness value in micrometers.

The microstructure of the paper surfaces was studied by the electron microscope JEOL JSM-5500LV, the samples were gold-coated.

In order to quantify SFE of the papers tested, four pure liquids — water (W, distilled water, pH 6.95), ethylene glycol (EG), formamide (FA) and methylene

iodide (MI) — were used. For each of these liquids the contact angle  $\theta_{eq}$  was determined. The characteristic parameters of all test liquids are shown in Table I (density  $\rho$ , viscosity  $\eta$ , surface tension and its components  $\gamma$  and volume of drop  $V_{drop}$ ).

Table I Physical parameters of standard set of liquids for dynamic contact angle measurement

Liquid	$\gamma_{LV}$ mN m <sup>-1</sup>	$\gamma_{LV^p}$ mN m <sup>-1</sup>	$\gamma_{LV^+}$ mN m <sup>-1</sup>	$\gamma_{LV^-}$ mN m <sup>-1</sup>	$V_{drop}$ $\mu$ l
W	72.8	51	25.5	25.5	10
EG	48	19	1.92	47	6.3
FA	58	19	2.28	39.6	7.5
MI	50.8	0	0	0	2.2

For contact angle measurement, KSV CAM 100 (KSV Instruments, Finland) was used. CAM 100 is a compact video-based instrument equipped with a CCD camera at the resolution of 640×480 pixels. The software included in this instrument allows recording of the projected images of a liquid drop on a solid substrate and calculating the apparent contact angles by fitting in the drop contour profile. The image of a “sessile” liquid drop was captured immediately after the drop was placed on the sample surface (time  $t = 0$ ) and afterwards every second during an interval of at least 20 s. A threaded plunger Hamilton syringe 1 ml (13.23  $\mu$ l per rotation) terminated by a stainless steel needle was used. The same micro-syringe was used for all liquids. The volume of the self-forming drop at the end of the needle varied according to the density and cohesion energy of the liquid. The distance from the substrate to the tip of the dosator ranged from 1 to 2 mm. When a liquid drop is sufficiently small and surface tension prevails over gravity, it is generally assumed that the drop forms a spherical cap shape. For the individual test liquids, a small drop deposited on the surface of a solid sample formed a spherical cap of the volume from 2 to 10  $\mu$ l ( $V_{drop}$  in Table I). At least three independent measurements were taken for every combination of the solid samples and test liquids. The contact angle measuring was carried out at room temperature (21-23 °C).

The model proposed in Refs [1-4], describing the time dependence of the cosine of DCA given by Eq. (6), was applied to the experimental data. The parameters  $A$ ,  $B$ ,  $k_1$  and  $k_2$  were estimated by non-linear regression; the minimization of the objective function was based on the least squares method. The estimates of all four parameters were statistically significant; the fit indicators showed very good results as well. The parameters resulting from the fit of the experimental data were used for the subsequent estimation of the contact angle  $\theta_{eq}$  [4].

For comparison, Arcotec test inks were used as a means of determining the surface energy value in practice. This testing method is quite suitable for the operating personnel at any production line as a routine check. The test inks (ISO 8296) are fluids of defined surface tension. The surface energy of a substrate is checked simply by applying the test ink to the surface. The accuracy of the measurement is  $\pm 1 \text{ mN m}^{-1}$ . The test inks were available in the standard range between 28 and 56  $\text{mN m}^{-1}$ .

## Results and Discussion

### Surface Microstructure and Roughness of Papers

The values of surface roughness measured on both sides, A and B, of the paper samples by a profilometer and the PPS instrument are summarized in Table II.

Table II Surface roughness of tested sets of Hello and Core papers

Paper sample		PPS $\mu\text{m}$	$R_a$ $\mu\text{m}$	$R_z$ $\mu\text{m}$
Hello Gloss	HG A	$1.19 \pm 0.06$	$0.29 \pm 0.05$	$1.08 \pm 0.59$
	HG B	$1.16 \pm 0.06$	$0.26 \pm 0.17$	$1.00 \pm 0.53$
Hello Silk	HS A	$1.78 \pm 0.06$	$0.43 \pm 0.30$	$1.98 \pm 1.78$
	HS B	$1.93 \pm 0.12$	$0.57 \pm 0.07$	$2.59 \pm 0.65$
Hello Matt	HM A	$2.17 \pm 0.04$	$0.49 \pm 0.01$	$2.04 \pm 0.23$
	HMB	$2.50 \pm 0.13$	$0.44 \pm 0.02$	$1.96 \pm 0.34$
Core Gloss	CG A	$1.25 \pm 0.02$	$0.36 \pm 0.14$	$1.40 \pm 0.03$
	CG B	$1.28 \pm 0.04$	$0.44 \pm 0.14$	$2.23 \pm 1.14$
Core Silk	CS A	$2.36 \pm 0.17$	$0.57 \pm 0.24$	$2.37 \pm 0.05$
	CS B	$2.62 \pm 0.13$	$0.84 \pm 0.48$	$3.02 \pm 1.31$
Core Uncoated	CU A	$6.19 \pm 0.33$	$2.32 \pm 0.86$	$8.00 \pm 2.34$
	CU B	$5.93 \pm 0.22$	$2.16 \pm 0.05$	$7.62 \pm 0.72$

The surface roughness data, measured by two different methods, correlate well with each other, the correlation coefficients  $R_a/PPS$  and  $R_z/PPS$  are equal to 0.977 and  $R_a/R_z$  to 0.996 (Fig. 1).

The electron microscopy images of the paper surface microstructure of all tested samples are presented in Fig. 2. It is obvious from these pictures that in this

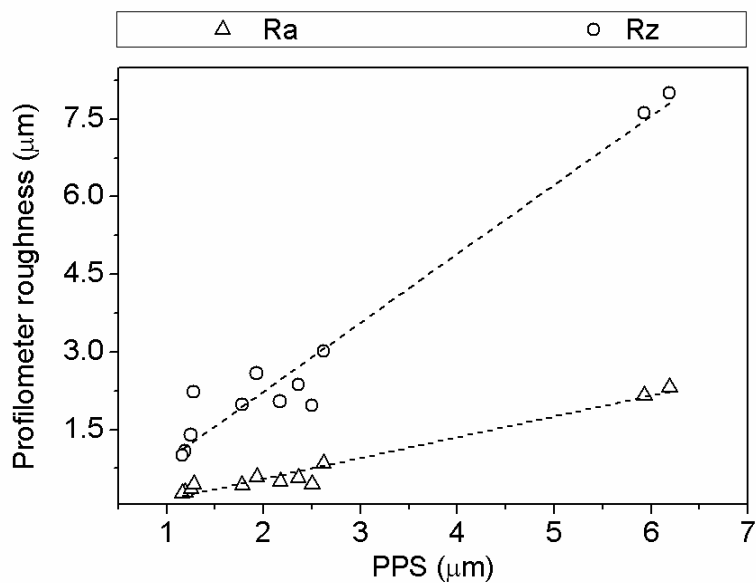
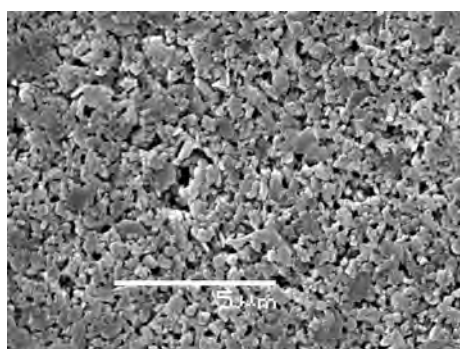


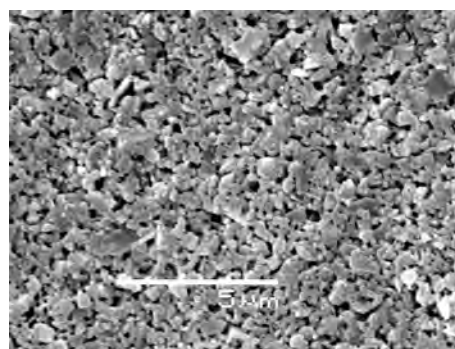
Fig. 1 Relation between the surface roughness of the tested papers measured by a profilometer ( $R_a$ ,  $R_z$ ) and by the PPS method

set of papers the greater roughness is achieved only by using a larger pigment particle size in the coating.

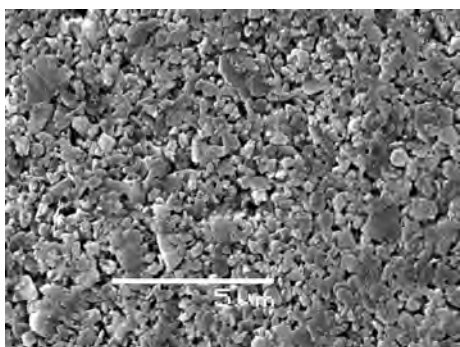
We observed that after the impact of the drop on the paper surface all tested liquids showed a gradual decrease of the contact angle, in some cases up to the or-



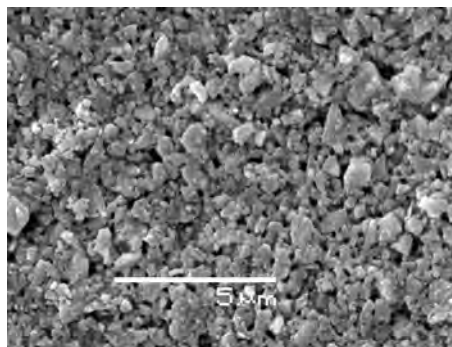
HG



CG

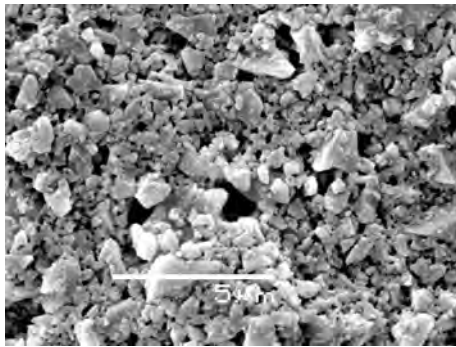


HS

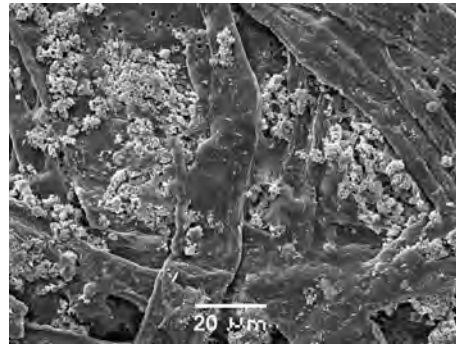


CS





HM



CU

Fig. 2 SEM images of the paper surfaces: HG -Hello Gloss, HS-Hello Silk, HM-Hello Matt, CG-Core Gloss, CS-Core Silk, CU-Core Uncoated.

der of 20 to 30 degrees, depending on the type of the substrate and the liquid. A more pronounced decrease was observed in samples of greater roughness and porosity, as can be seen in Fig. 3 which shows the typical course of DCA of water and methylene iodide drops on a set of Hello papers.

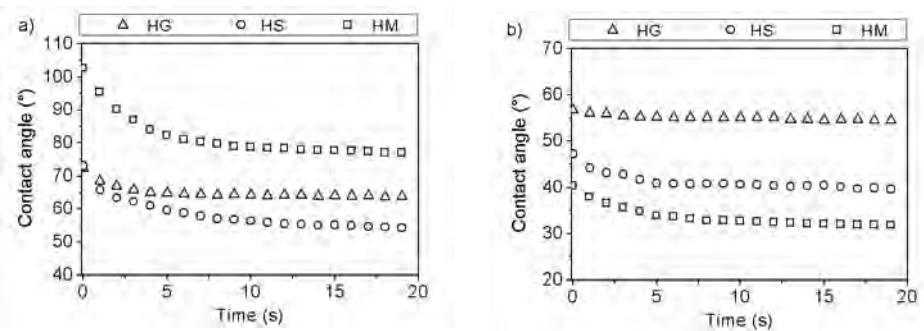


Fig. 3 Time dependence of the contact angle of water (a) and methylene iodide (b) drops on papers Hello Gloss (HG; PPS 1.19  $\mu\text{m}$ ), Hello Silk (HS; PPS 1.93  $\mu\text{m}$ ) and Hello Matt (HM; PPS 2.17  $\mu\text{m}$ )

When using the “ $\cos \theta$ ” model [1-4] describing the behaviour of droplets on a non-ideal surface in the respective time region as two phases — a relatively quick phase when the spreading of the liquid dominates, the rate parameter being  $k_1$ , and a slower phase when the drop volume decreases due to penetration (and/or evaporation) of the liquid into the solid, with the rate parameter  $k_2$  — the effect of surface roughness of the tested samples can be characterized. As shown in Fig. 4a, the rate of spreading of water decreases with the increasing micro-roughness of the papers (correlation coefficient equal to  $-0.912$ ). The penetration rate of water (the rate constant  $k_2$ , Fig. 4b) increases with the increasing roughness (correlation coefficient  $0.936$ ). This is in agreement with the change in topography, the growing size of the particles and the diversity in the shapes of the pigments in the coating

layer and, therefore, significantly greater surface porosity as compared with gloss papers (see EM images in Fig. 2). A similar behaviour was also observed using other standard liquids.

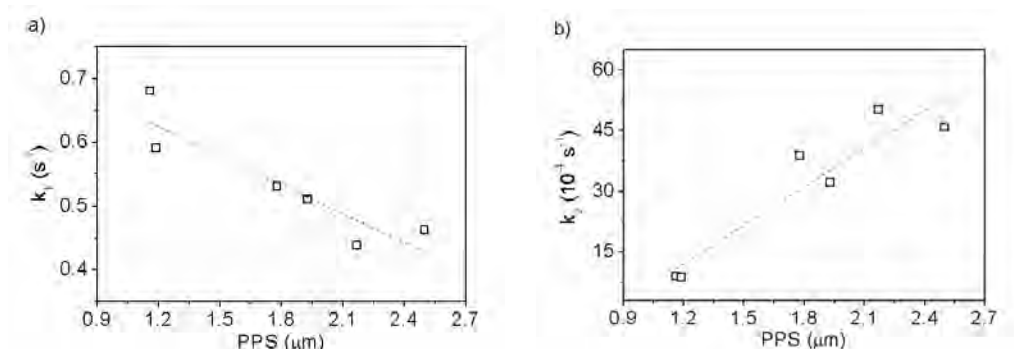


Fig. 4 The effect of PPS roughness of Hello papers on the rate parameter of water spreading  $k_1$  (a) and the rate parameter of water penetration into the coating layer  $k_2$  (b)

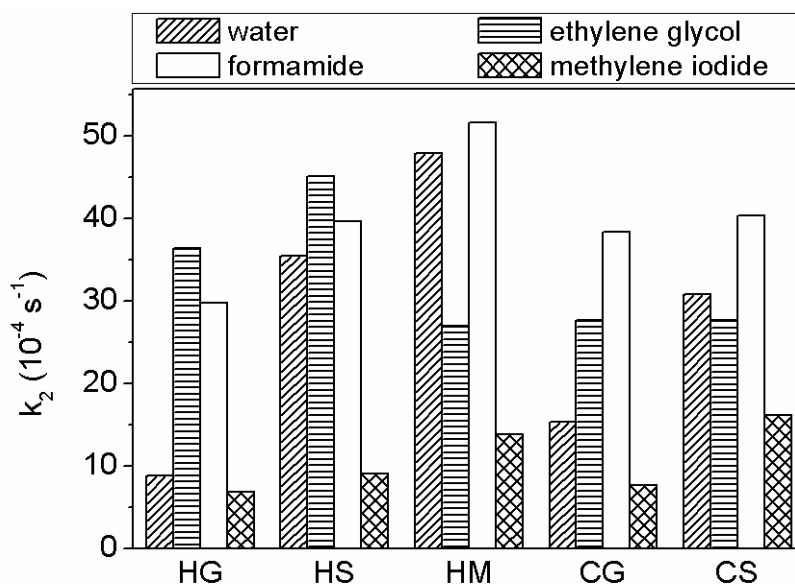


Fig. 5 Rate parameters  $k_2$  expressing the penetration of standard liquids into the tested coated paper surfaces (HG, HS and HM Hello papers, CG and CS Core papers)

The rate parameter  $k_2$  indicates the ability of liquids to penetrate into the surface layer of coated papers, allowing to quantify the absorption of various liquids. The ability of coated papers of the same type produced by different manufacturers to absorb liquids is reflected in their differing values of  $k_2$ . The values of  $k_2$ , averaged for both sides of the papers (Fig. 5), prove significantly higher absorption of formamide and ethylene glycol than that of methylene iodide.

Interesting results were obtained when comparing the  $k_2$  values of standard

liquids for uncoated (CU) and gloss coated papers (CG) of the Core series. The value of  $k_2$  for water on uncoated paper was negative, as the contact angle after the spreading phase slowly grew, probably due to the swelling of naked cellulose fibres on the surface (see SEM in Fig. 2). The rate parameter of penetration  $k_2$  for ethylene glycol on uncoated CU paper was about 0.3 times lower, for formamide 3 times higher and for methylene glycol 9 times higher than on coated glossy paper CG. It was due not only to the effect of different surface roughness, but rather to the more heterogeneous chemical composition of the surface (see SEM in Fig. 2).

The pseudo-equilibrium contact angle is determined by both the partial processes on which the surface roughness has a completely contradictory influence (see Fig. 4). The rate parameter of spreading  $k_1$  decreases with the increasing roughness and the difference between the initial and the equilibrium contact angle also increases. If the rate parameter of penetration of the liquid does not grow markedly with the increasing roughness, the contact angle  $\theta_{eq}$  decreases with the increasing paper roughness, as in the case of methylene iodide shown in Fig. 6. If the liquid penetration rate increases significantly at a roughness above a certain limit value, this process can prevail, the spreading is completed within a shorter time and a steady state is achieved on a rough surface at a higher value of the contact angle than on a smooth surface, as in the case of water on coated papers with PPS roughness greater than  $\sim 2 \mu\text{m}$  (Fig. 6).

On the basis of the “cos  $\theta$ ” model [1-4], the values of  $\theta_{eq}$  for four test liquids on all tested paper samples were determined. Subsequently the surface free energy

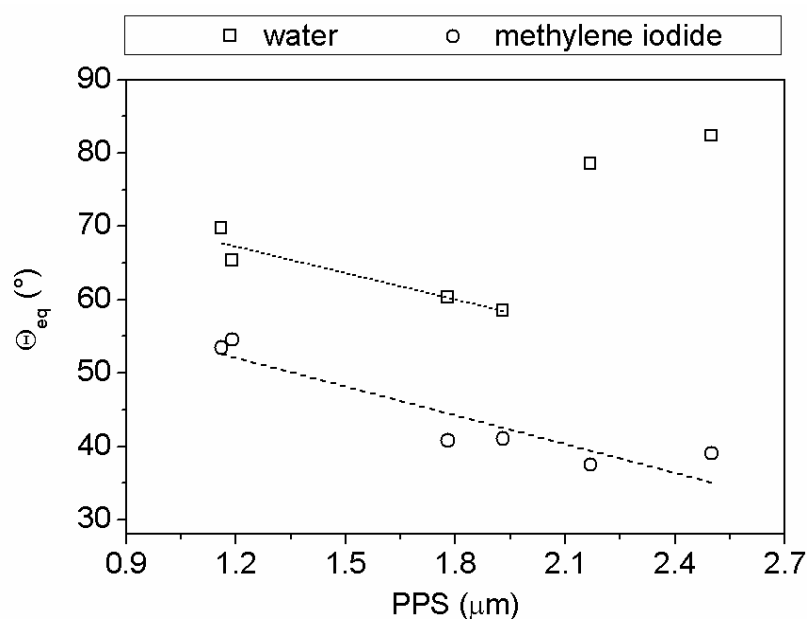


Fig. 6 Pseudo-equilibrium contact angle  $\theta_{eq}$  of water and methylene iodide on Hello papers with different PPS roughness

of papers was calculated as  $\gamma_{SV}$  by the Oss, Good and Chaudhury, Owens–Wendt and Wu methods, starting from the same values of contact angles.

Table III Surface free energy (*SFE*) of papers tested, calculated according to various approach to evaluation of interfacial solid/liquid tension according to Oss, Good and Chaudhury (OGC, Eq. (3)), Owens–Wendt (OW, Eq. (1)) and Wu methods (Wu, Eq. (2))

Paper sample		Calculation method of <i>SFE</i>					
		OGC		OW		Wu	
		<i>SFE</i> mJ m <sup>-2</sup>	Polar component %	<i>SFE</i> mJ m <sup>-2</sup>	Polar component %	<i>SFE</i> mJ m <sup>-2</sup>	Polar component %
Hello Gloss	HG A	35.8	9.7	42.5	23.5	42.0	19.7
	HG B	33.7	6.1	41.1	31.2	42.0	21.0
Hello Silk	HS A	51.3	22.4	47.3	23.3	46.9	15.1
	HS B	49.3	20.8	52.6	25.7	46.6	14.9
Hello Matt	HM A	43.2	5.4	43.2	10.7	47.1	12.2
	HMB	42.9	6.7	42.9	8.5	46.7	13.0
Core Gloss	CG A	40.4	19.3	43.3	25.5	40.2	16.8
	CG B	38.5	3.5	39.8	6.3	41.7	8.7
Core Silk	CS A	25.6	0.9	27.3	3.8	30.1	6.9
	CS B	33.3	6.3	27.8	4.0	31.8	4.5
Core Uncoated	CU A	40.5	6.3	44.9	4.0	45.1	4.5
	CU B	44.7	3.2	43.1	3.3	48.5	11.8

The SFE values presented in Table III show diverse values of both the individual components and the total values of SFE, which appear to be rather little correlated if calculated according to the individual theories as shown in Table IV. The total values of SFE calculated using the OGC method were predominantly lower than the values determined by the other methods (Fig. 7). The dispersion components calculated on the basis of Eqs (1)-(3) seem to have a better match than the polar

components of SFE. The average values of the polar components of SFE of coated papers according to the OGC method were only 4.4 %, as against the values calculated by the other methods (16.2 % for OW and 13.3 % for Wu).

Table IV Correlation coefficients of the data fields represented by the values of SFE and its components calculated according to the three different evaluation methods (see Table III)

Data fields		Correlation coefficients		
		OGC/OW	OGC/Wu	OW/Wu
SFE total		0.859	0.844	0.920
SFE components	polar	0.729	0.459	0.834
	dispersion	0.905	0.987	0.931

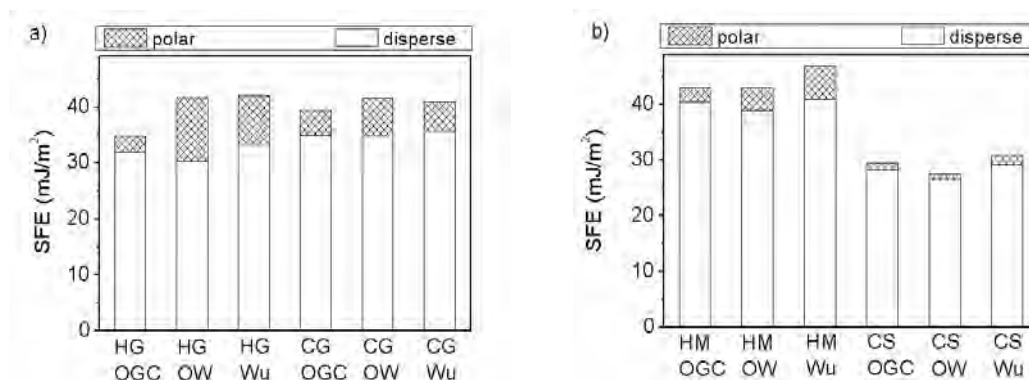


Fig. 7 Demonstration of the different methods of calculation of the values of SFE and its components (the van Oss, Good and Chaudhury (OGC, Eq. (3)), Owens–Wendt (OW, Eq.(1)) and Wu methods (Eq.(2)) for gloss coated papers with PPS ~ 1.2 μm (a) and silk and matt papers with PPS ~ 2.4 μm (b)

The use of test inks (e.g., Arcotec inks) to determine SFE by the method used in the printing practice has led to values that are very insensitive to the surface roughness of coated papers (this method was inapplicable to uncoated paper). The values we obtained for HG and CG papers were 32 mJ m<sup>-2</sup>, for HS, HM, and CS papers 35 mJ m<sup>-2</sup>.

## Conclusion

Pigment coatings improve the printing properties of papers. The top surface layer influences strongly the printing performance, as this is where the ink first makes contact. The method of monitoring the behaviour of the drop of a liquid on the surface of a paper in the time region of tens of seconds after the drop impact (the dynamic contact angle) allows not only to determine the surface free energy of the paper, but also provides a range of other information concerning the liquid/paper interaction. Evaluation of the time dependence of the liquid drop contact angle using the “ $\cos \theta$ ” model [1, 4] provides not only the pseudo-equilibrium contact angle  $\theta_{eq}$ , necessary for the calculation of SFE, but also the rate parameters of the spreading  $k_1$  and of the penetration of the liquid into the surface coating layer  $k_2$ . The same experimental method can be used to monitor the interactions of non-standard liquids, such as liquid inks, varnishes or adhesives, with the surface of printing substrates (papers, foils).

Surface roughness affects the behaviour of a liquid on the surface of the printing paper through two concurrent processes, of liquid spreading and liquid penetration. Papers of the same PPS roughness may exhibit different values of SFE and may appear slightly different in the printing processes. The numerical value of SFE depends very substantially on the method of calculation, i.e. on the theoretical approach used to describe the interphase interactions (the values calculated according to the OGC method are mostly lower than those calculated according to other methods). When assessing a range of materials, therefore, one should be especially careful to interpret the experimental data correctly.

## Acknowledgements

*This work was supported by the Ministry of Education, Youth and Sports of the Czech Republic; research project No. MSM 0021627 501.*

## References

- [1] Kaplanová M., Otáhalová L., Muck, T.: Adv.Print. Media Technol. **35**, 213 (2008).
- [2] Kaplanová M., Hejduk J.: *Influence of Rubber Surface Tension on Ink Transfer in Flexography*, Conference Proceedings of Printing Technology

- SPb '06, 26–30 June 2006, St. Petersburg, Russia, 2006.
- [3] Kaplanová M., Hejduk J., Panák O.: *Adv. Print. Media Technol.* **36**, 309 (2009).
  - [4] Kaplanová M., Syrový T., Držková M., Syrová, L.: *J. Mater. Sci.* – submitted.
  - [5] De Gennes P., G.: *Rev. Mod. Phys.* **57**, *Wetting: Statics and Dynamics*, 827 (1985).
  - [6] Erbil H., Y.: *Surface Chemistry of Solid and Liquid Interfaces*, Blackwell Publishing, 2006.
  - [7] Owen J.: *Surface Energy* in: *Comprehensive Desk Reference of Polymer Characterization and Analysis*, Brady R.F., Jr. ed., Oxford University Press, 361-374, 2002.
  - [8] Seveno D., Dinter N., De Coninck J.: *Langmuir* **26**, 14642 (2010).
  - [9] Mittal K.L., ed., *Contact Angle. Wettability and Adhesion*, VSP Utrecht, The Netherlands, 1993.
  - [10] Blake T.D.: *J. Colloid. Interface Sci.* **299**, 1 (2006).
  - [11] Liukkonen A.: *Scanning* **19**, 411 (1997).